Transactions, **SMiRT-26**
Berlin/Potsdam, Germany, July 10-15, 2022
Division III

Investigating the shear performance of SC walls under impact loads

Ahmed Elhattab[1], Derrick Watkins[2], Randy James[3], Rim Nayal[4], Amber Berger[5], and Josh Parker[6]

[1] Senior Engineer II, SC Solutions, Inc., Sacramento, CA, USA (aelhattab@scsolutions.com)
[2] Vice President – Structures, SC Solutions, Inc., Sacramento, CA, USA
[3] Principal, Structural Solutions Consulting, LLC., San Diego, CA, USA
[4] Civil/Structural Engineer 4, NuScale Power, Corvallis, OR, USA
[5] Supervisor, Civil/Structural Design. NuScale Power, Corvallis, OR, USA
[6] Lead Supervisor, Civil/Structural Design. NuScale Power, Corvallis, OR, USA

ABSTRACT

Steel-plate composite (SC) structures consist of infilled concrete between steel faceplates with shear ties connecting the front and back faceplates. Shear ties can be made of bars, rebars, plates, or steel shapes. Currently, there is a tendency in the nuclear industry towards utilizing plate shear ties since they provide better handling performance of the skeletal steel modules during construction. The "smooth" interface for plate ties does not provide sufficient bonding to the concrete which reduces the panel shear performance. Additionally, the unidirectional orientation of the shear tie plates introduces orthotropic out-of-plane shear capacity for the panel where one orientation observes a nonductile shear failure in the concrete "cell' bounded by two shear plates, while the other orientation observes flexural-shear failure in the shear ties. Previous studies investigated the out-of-plane shear performance of SC panels for design-based loads (using experimental data for quasi-static four point bending tests). However, there is scarcity in the research that investigates the out-of-plane shear performance for beyond design basis events such as Aircraft Impact. This paper presents results of an analytical study investigating the shear performance at connections in SC structures for high-speed impact loading. First, detailed FE models are benchmarked to test data to establish a valid modelling approach for SC panels. The proposed modelling approach is then expanded to high-speed impact shear loading case to assess the effectiveness of different shear tie configurations (rebar-type versus plate-type reinforcement) in meeting regulatory requirements for aircraft impact.

INTRODUCTION

Steel-plates composite (SC) structures, using infilled concrete between steel faceplates, are becoming more and more common in next generation nuclear facilities. The main interest in using Steel-plates composite (SC) walls is its modular construction system, which provides a much faster erection and construction system compared to conventional Reinforced Concrete (RC) walls. This flexibility has the potential to reduce plant construction schedule and cost (Sener & Varma, 2021). Accordingly, there has been a great research interest on understanding the behaviour of SC walls under different loading conditions.

The components of the SC wall system are presented in Figure 1. The outer steel liners or face plates are anchored to the concrete matrix with steel headed studs. The tie plates connect the steel face plates to provide stability during construction and to enhance the workability and handling of the modules. In this system, the steel liners replace compression/tension rebar layers. The studs resist the shear flow that develops at the interface layer between the concrete and the steel liners. The concrete infill and the rib tie plates are the main systems resisting the out of plane shear on the wall.

Recently, researchers have investigated the out of plane shear behaviour of SC walls under quasi-static loading. Sener et. al. (2016) have conducted experimental and numerical investigation to evaluate the out of plane behaviour of SC walls without shear reinforcement. The study investigated the effect of different parameters on the behaviour of the SC walls including the 1) stud spacing, 2) the shear-span-to-depth ratio, and the 3) face plate reinforcement ratio. The results showed that the lower bound for the out of plane shear capacity presents when the shear span to depth ratio is higher than 3 (Japanese Electric Association, 2005; Sener et al., 2016). While, at lower span-to-depth ratios the SC wall behaves as a deep beam where the load is transferred through a strut-tie model, and the SC wall shows higher shear resistance. The study also showed that the contribution of the face plate dowel action has almost negligible effect on the shear capacity of the section. In continuation of this effort, Sener et. al. (2021) expanded their study by investigating SC walls with different types of out-of-plane shear reinforcement. They tested two different types of shear reinforcement: 1) rebar type shear reinforcement, and 2) plate (diaphragm) type shear reinforcement. Two configurations were investigated for the plate type shear reinforcement: a) the plate (diaphragm) runs parallel to the shear plane, and b) the plate (diaphragm) runs perpendicular to the shear plane. The study validated the AISC N690 code equations for out of plane shear capacity utilizing experimental test data and numerical models. In all cases (except for one case) the AISC N690 code equations provided adequate estimates of the shear strength (mean value for the ratio of experimental shear capacity/AISC-N690 nominal shear capacity is 1.34). Only for plate type shear reinforcement with plate (diaphragm) running perpendicular to the shear plane, the AISC-N690 conservatively underestimates the shear capacity of the section. Sener et. al. (2021) proposed an alternative approach by smearing out the shear reinforcement plate into an equivalent continuous web plate. The contribution of the steel in the shear strength is then calculated as the web plate shear yield strength. The proposed approach showed a better estimation for the shear strength when compared to the experimental and numerical data. Further research has also been conducted to assess the effect of membrane forces on the out of plane shear capacity, and the effect of cyclic loading on degrading the out of plane shear stiffness (Sener et al., 2015; Varma et al., 2014). However, there is a scarcity on the research that investigate the out of plane shear performance of SC walls under highspeed impact.

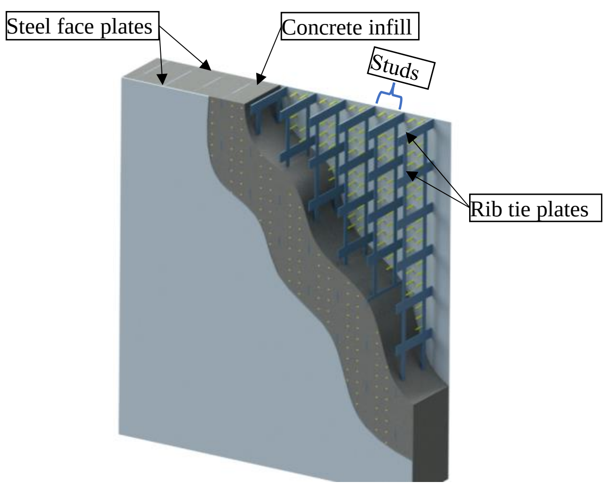

Figure 1. Steel composite plates

The out of plane shear performance of steel composite walls is essential when conducting large commercial aircraft impact assessment for reactor buildings. After the September 11th, 2001, terrorist attack in the United States, the US NRC (Nuclear Regulatory Commission) required that any new Nuclear Power Plant (NPP) facility must conduct an Aircraft Impact Assessment (AIA) for the NPP structural system. The main objective of the analysis is to identify and incorporate design features and functional capabilities to show that, with reduced use of operator actions, the reactor core remains cooled and the spent fuel cooling or spent fuel pool integrity is maintained. This can be achieved by preventing perforation of containment building walls. Extensive damage is allowed; however, the damage should not allow fire or debris to enter critical areas of the building. For these assessments, the impact location in the AIA analyses should be chosen to maximize the bending and shear straining actions in the impacted walls. Over the past decade, there has been multiple research studies that investigated the flexural performance of SC walls under high-speed impact loads (Brown et al., 2012; Mizuno, Koshika, Morikawa, et al., 2005; Mizuno, Koshika, Sawamoto, et al., 2005; Mizuno, Koshika, Tanaka, et al., 2005; Woodfin, 1983). However, there is a scarcity in the literature which investigate the shear performance of SC walls under impact load.

The overarching goal of this paper is to compare the performance of different shear reinforcement configurations in SC walls under high-speed impact loads. Particularly, the paper will compare the round rebar type shear reinforcement to the plate type shear reinforcement. The paper will adopt a numerical approach to conduct this study, using explicit finite element modelling approach using LS-DYNA software. To validate the modelling approach, the paper commences by validating the numerical material constitutive model using lab test data. The validation was carried out using quasi-static experiment data and using high speed impact test data. Afterward, the validated models will be used to assess the performance of SC walls with different types of shear reinforcement under quasi-static loading and high-speed impact loading. The study will compare the performance for different configurations for the same shear reinforcement ratio, while maintaining other parameters constant such as shear span to depth ratio, studs' reinforcement ratio, and steel plate reinforcement ratio.

NUMERICAL MODEL VALIDATION

The scope of this section is to validate the shear behaviour of the concrete and steel elements and material constitutive models. Since the analysis will be carried out for high-speed impact loading, the validation procedure will be performed in two stages. The first stage will validate the shear behaviour of the material constitutive models and associated finite element modelling approach using quasi-static laboratory test data. Four cases will be studied:

1) Steel Composite wall without shear reinforcement (Test #1)
2) Steel Composite wall with rebar type shear reinforcement (Test #2)
3) Steel Composite wall with plate type shear reinforcement:
    a. Shear plane is parallel to the diaphragm plates (Test #3)
    b. Shear plane is perpendicular to the diaphragm plates (Test #4)

The test data for these experiments are based on the work done by Sener et. al. (2021). The scope of this validation is to establish that the numerical modelling approach can adequately predict the shear capacities of different types of SC walls.

The second stage will validate the flexural and punching/shear failure behaviour of the material constitutive models under high speed impact loading using experimental test data conducted by Mizuno et. al. (2005). It is essential to note that the type of failure in this experiment is a two-way shear failure which is different from the one-way shear failure that is investigated in this paper. However, as previously mentioned, to date there is no available experimental data that investigated the performance of one-way shear in SC walls under impact loading. Additionally, the proposed validation framework should provide a best estimate for the material behaviour which can be used to predict the performance of the wall under one way shear. Two cases will be studied:

1) Impact with 80mm thick SC panel: to validate the flexural behaviour SC panel
2) Impact with 60mm thick SC panel: to validate the punching shear behaviour of the SC panel

Validating the material constitutive model using quasi-static loading

The four experimental tests that will be used in this validation procedure are presented in Figure 2, extracted from the work done by Sener et. al. (2021). All specimens were subjected to four point bending load. The concrete properties, reinforcement ratios, shear span to depth ratio ($\frac{M_u}{V_u d}$), and the shear strength of the sample ($V_{u\ exp}$) are summarized in Table 1. The suite of test data will validate the capability of the material constitutive model to predict the shear failure behaviour of:

1) Test #1: SC walls without shear reinforcement (plain concrete shear strength)
2) Test #2: SC walls with round rebar shear reinforcement
3) Test #3: SC walls with plate type shear reinforcement (shear plane is parallel to the shear diaphragm)
4) Test #4: SC walls with plate rebar shear reinforcement (shear plane is perpendicular to the diaphragm)

Table 1: Properties of the SC samples

Test	Shear reinforcement type	d (in)	L/d	b_w/d	t_p (in)	$\rho_p = \frac{2t_p}{d}\%$	$\frac{M_u}{V_u d}$	$\frac{s}{t_p}$	d_{stud} (in)	$\rho_s = \frac{A_{stud}}{s_L s_T}\%$	$\frac{S}{d}$	$\rho_s = \frac{A_{Tie}}{s_L s_T}\%$	fc' (ksi)	$f_{y\ plates}$ (ksi)	$f_{u\ studs}$ (ksi)	$f_{y\ ties}$ (ksi)	Reference specimen	$V_{u\ exp}$ (kips)
Test #1	No reinforcement	36	11	0.95	0.5	2.78	3.2	20	0.75	0.39	NA	NA	6.2	71	75.5	NA	SP1-5*	185
Test #2	Rebar type	36	11	0.95	0.75	4.2	3.5	11.3	0.75	0.62	0.47	0.15	7	58	75.5	93.6	SP2-a-1**	364.4
Test #3	Plate Type: Diaphragm is parallel to shear plane	17.7	9	1	0.39	4.4	2	15	0.75	1.27	1	0.9	4.3	60.2	75.5	60.2	SP2-d-1**	181.2
Test #4	Plate Type: Diaphragm is perp. to shear plane	17.7	10	2	0.39	4.4	2	15	0.75	1.27	0.9	0.74	4.34	60.2	75.5	60.2	SP2-d-2**	525.4

* Sener et. al. (2016) **Sener et. al. (2021)

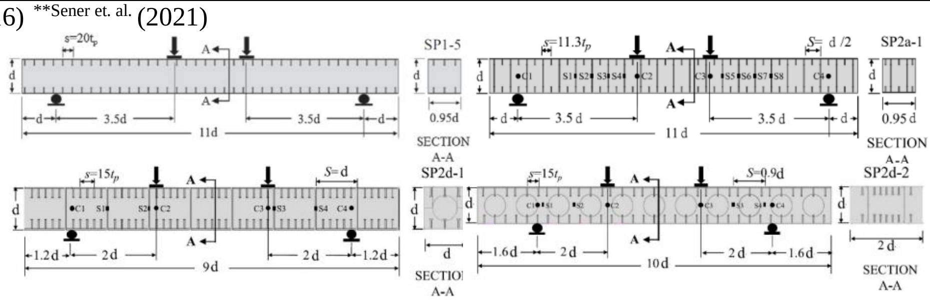

Figure 2. Configuration and dimensions of test problems (figure from Sener et. al. (2021))

The Finite Element Model (FEM) was developed using the LS-DYNA software. The concrete material was modelled using Winfrith smeared cracked model. The Winfrith material model was developed by DRASTIC (1986) to simulate the concrete behaviour under blast and impact loading. The material model is linear material with a failure surface fitted by Ottosen (Ottosen, 1975) failure surface. The material can depict three failure modes: compression, shear and tension. For compression and shear failure the material follows an elastic perfectly plastic surface cap, for tension failure the material follows a strain softening rule defined as a function of the concrete fracture energy. The material model also has a strain rate effect function that can be activated by the user. The steel was modelled using a piece-wise linear plasticity model (MAT-024). Frictional contacts have been used between the face plates shell elements and the concrete brick elements. For the selected suite of problems, the failure is driven by one-way shear in the concrete and the shear reinforcement. The model discretization was selected through several iterations using different mesh sizes. The FE models for Test 1 through 4 are presented in Figure 3. The load was applied in a displacement-controlled loading attribute using prescribed motion applied to the loading plates. Frictional contact was also used to define the contact between the loading plates and the supports with the faceplates.

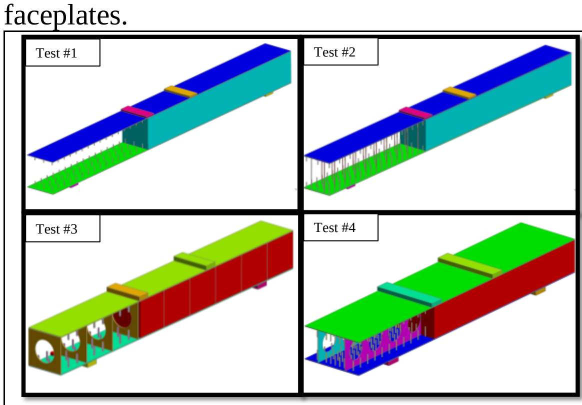

Figure 3. FE model for Test 1 through Test 4

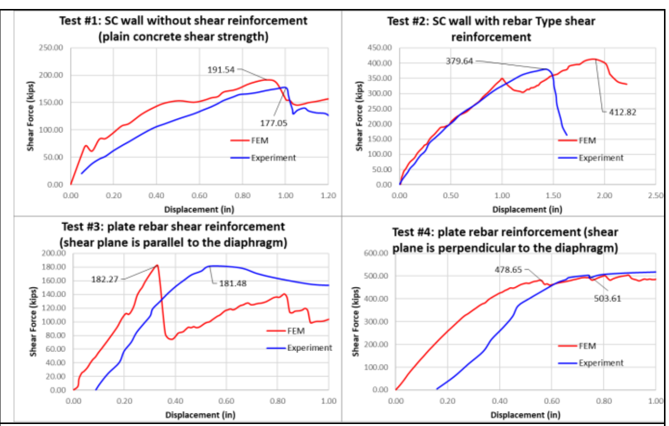

Figure 4. Compare shear force versus displacement plots for the experiment and the FE models

Shear force versus mid-span displacement history for all 4 models have been plotted against the experimental data and presented in Figure 4. Collectively, the concrete material constitutive model succeeded in predicting the peak strength for different types of steel composite walls. Also, the stiffness of the wall, represented in the slope of the loading curve, has been adequately captured by the Winfrith material constitutive model and the selected steel material model. In Test 1, 3, and 4 the specimen in the laboratory was initially subjected to cyclic loading to reach the cracked section stage before subjecting the full test load. That is reflected in the load displacement curves in two items: 1) FE models start with higher slope (stiffness) compared to experimental data 2) FE models start from zero displacement while experimental data are offset by the amount of deflection reached at the end of the pre-loading stage. The failure mode in all tests was shear failure which have been predicted by the FE model.

Validating the material constitutive model for impact loading

In this section, the selected material models and modelling approach are validated for high-speed impact using Mizuno et. al. (2005) experimental test data. The experiment consists of two steel composite panels that are subjected to missile impact at speed of 330 mph. The panel configuration is presented in Figure 5. The panel is constrained in the y-direction around its periphery with a thick steel beam which is 11.8” wide. The properties for the two tested panels are presented in Table 2. The load has been applied as a pressure time history on the steel face plates using the Riera function presented in Figure 5 (Mizuno, Koshika, Morikawa, et al., 2005; Mizuno, Koshika, Sawamoto, et al., 2005; Mizuno, Koshika, Tanaka, et al., 2005).

The steel composite panel was modelled using the same approach. The steel plates were modelled using the same piece wise linear plasticity material model and the concrete using winfrith material model. However, the yield strength for the studs and the steel plates was increased by 10% to account for the dynamic increase factor (DIF) (Mizuno, Koshika, Sawamoto, et al., 2005).

The 60mm panel fails by perforation at 7msec as presented in Figure 6, while the 80mm panel was not perforated. These observations align with the experimental results. The back face displacement was extracted from the FE model for both the 60mm and 80mm panels. The FE model results are compared to the experimental data as presented in Figure 7. The model adequately captured the pre-failure behaviour for the 60mm panel, as well as the peak deformation for the 80mm panel.

The validation problems show the capability of Winfrith material constitutive model and steel material model in capturing the performance of different type of SC walls under static and high-speed impact loads. These material models will be used in the following sections to assess the performance of different type of shear reinforcement under high-speed impact loads.

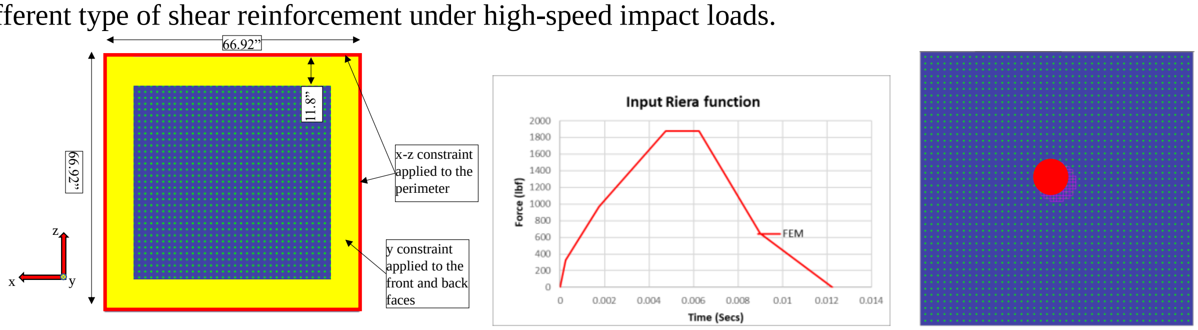

(a) (b) (c)

Figure 5. (a) Steel composite panel for Mizuno test (a) applied load time history (b) loaded area

Table 2: Properties of the SC panels

Test	Wall thickness (mm)	Panel dimensions (in)	Stud spacing (in)	t_p (mm)	$\rho_p = \frac{2t_p}{d}\%$	fc' (ksi)	$f_{y\ plates}$ (ksi)	$f_{y\ studs}$ (ksi)
Impact #1	80	66.92"×66.92"	1.57	1.2	3	5.74	50	50
Impact #2	60	66.92"×66.92"	1.57	0.8	2.67	5.47	50	50

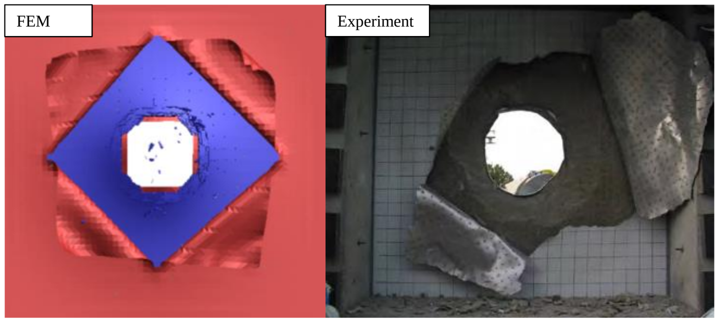

Figure 6. Compare damage in the SC wall for Impact #2 test

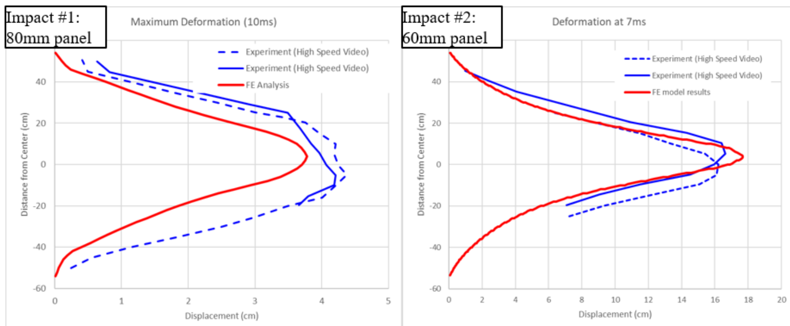

Figure 7. Compare FEM back face plate deflection over wall hight with the experimental data

SHEAR PERFORMANCE OF REBAR TIES VERSUS PLATE-TYPE SHEAR TIES

Assess the performance under quasi-static loading

A numerical model for a 5ft thick steel composite wall will be used to assess the performance of shear reinforcement. The wall configuration is presented in Figure 8. This configuration is typical for new nuclear construction. As presented in the figure, at the supports, a continuity solid plate is added. The continuity plate resembles the connection at the wall corners, particularly at the wall-to-wall connection. To maintain adequate bonding between the concrete on both sides of the continuity plate, studs were used on both sides. Section A-A shows a cross section in the SC wall, as shown in the section the faceplates are reinforced with 4x4 angles spaced every 24". The property of each SC wall is presented in Table 3. SC-1 has a plate type shear reinforcement consists of 0.75″x10″ tie plates connected with two transverse 4″ plates as presented in Figure 8. The shear reinforcement in SC-2 consists of 1″ rebar tie rods spaced every 8" in the two orthogonal directions. The two walls have the similar reinforcement ratio and shear strength based on AISC-N690 and ACI 349 equations.

The numerical modelling approach has been used to estimate the shear strength of the wall under quasi-static loading. The analysis was carried out using explicit solver with adequate damping assigned to the model (30% of the system critical damping) to maintain the ratio of the kinetic energy to internal energy less than 4% throughout the analysis time. The shear span to depth ratio is 3.5 for the two walls. The shear force versus midpoint displacement plot is presented in Figure 11. The wall section is controlled by flexural failure ($M_n \approx 100 \times 10^3 kip.ft$), therefore the load displacement relation plateaus when the face plates reach the yield strength. The wall continues to transfer load till the maximum shear capacity is reached when the load curve starts to drop. The nominal shear capacity calculated with ACI 349 and AISC N690 equations are also plotted in the figure. The models adequately capture the wall shear capacity. Figure 9 and Figure 10 present the shear damage at the point of failure. SC-1 wall failed by forming a compression strut in the "concrete cell" bounded by the face plates. This type of damage is similar to the damage observed in the laboratory test conducted by Sener et. al. (2021). The maximum principal strain at plate type rib ties reached 3.5%, and no failure was observed in the rib ties. SC-2 sample failed by forming a 45°

compression strut in the shear zone. Multiple shear ties were ruptured at the end of the analysis. Similarly, the shear crack map from the FE model aligns with the shear crack map for an SC-wall reinforced with rebar type in the work done by Sener et. al. (2021) as presented in Figure 10.

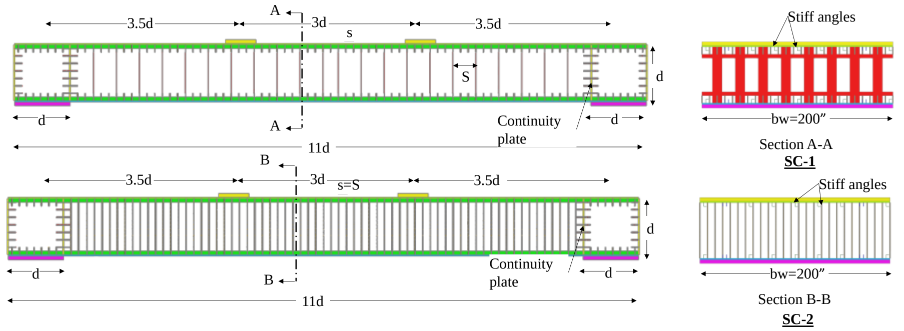

Figure 8. Configuration of the 5ft thick steel composite wall

Table 3: Properties of the SC samples

Test	Shear reinf. type	d (in)	L/d	b_w/d	t_p (in)	$\rho_p = \frac{2t_p}{d}\%$	$\frac{M_u}{V_u d}$	$\frac{s}{t_p}$	d_{stud} (in)	$\rho_s = \frac{A_{stud}}{s_L s_T}\%$	$\frac{S}{d}$	$\rho_{SV} = \frac{A_{Tie}}{S_L S_T}\%$	fc' (ksi)	$f_{y\ plates}$ (ksi)	$f_{u\ studs}$ (ksi)	$f_{y\ ties}$ (ksi)	$V_{n\ AISC}$ N690 (kips)	$V_{n\ ACI}$ 349 (kips)	$V_{FE}/V_{n\ AISC}$ N690	$V_{FE}/V_{n\ ACI}$ 349
SC-1	Plate type	60	11	3.33	0.75	2.5	3.5	10.6	1	1.2	0.4	1.3	5	65	45	65	9200	11250	1.15	0.95
SC-2	Rebar type	60	11	3.33	0.75	2.5	3.5	10.6	1	1.2	0.13	1.27	5	65	45	65	8700	10300	1.16	0.98

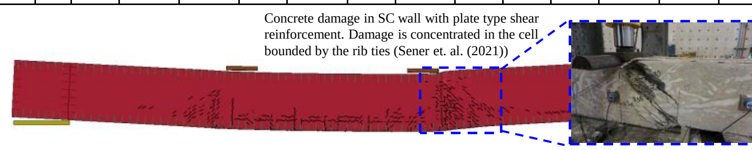

Figure 9. Shear damage in the FE model for SC-1 wall at end of analysis compared to experimental record for a similar SC wall

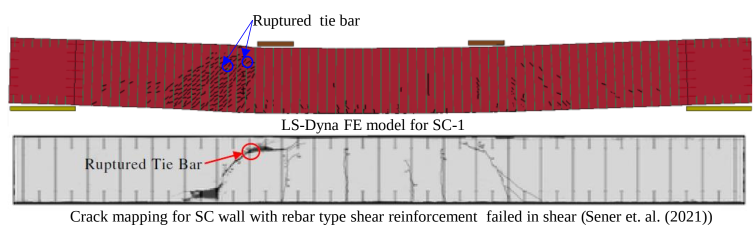

Figure 10. Shear damage in the FE model for SC-2 wall at end of analysis compared to experimental record for a similar SC wall

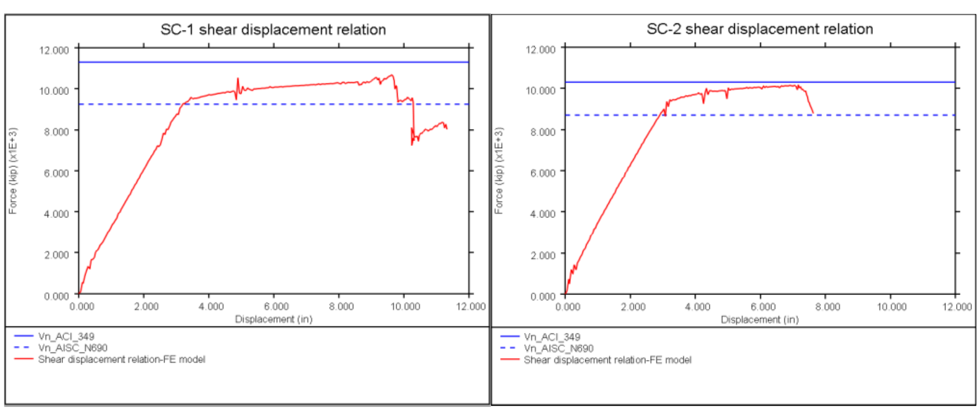

Figure 11. Force displacement relation

Assess the performance under high-speed impact loading

To evaluate the performance of the SC walls under high-speed impact loading, the wall model was modified to simulate the wall-to-wall connection configuration as presented in Figure 12. The loading function is developed for a water slug with 8ft diameter, 8ft long and impact the at 335mph. This load configuration is found to be the maximum that the SC-2 can sustain. The load is applied as a variable pressure time history using a Riera function. The Riera function is presented in Figure 12, as shown the load is applied right at the beginning of the wall-to-wall connection to maximize the shear damage.

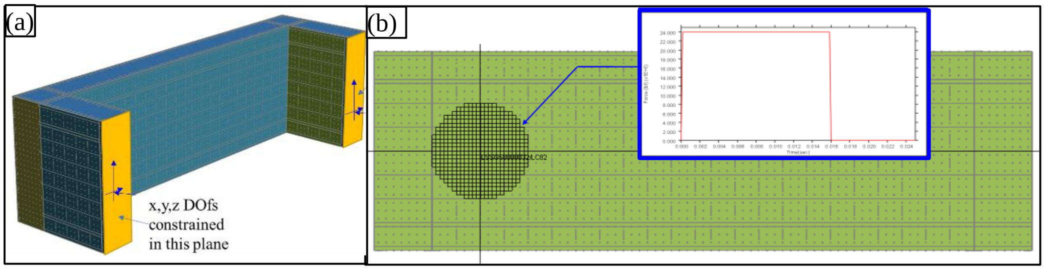

Figure 12. Model assignments (a) boundary conditions (b) applied pressure time history

Figure 13 presents the damage on the two walls at the end of the simulation time. SC-1 could not sustain the applied load, the wall shows a severe shear damage at the wall-to-wall connection. The wall has been tested by applying the impact load at mid-span to assure that the wall failure is not driven by flexural mode. The walls (SC-1 and SC-2) successfully sustained the applied load when the load is applied at mid-span. It is essential to highlight that the current approach for meeting the regulatory requirements for aircraft impact is to prevent any pressurized fire or debris from entering the containment building. This is achieved by preventing any through wall cracks in the containment building walls. As presented in the figure the plate type shear reinforcement did not achieve that requirement.

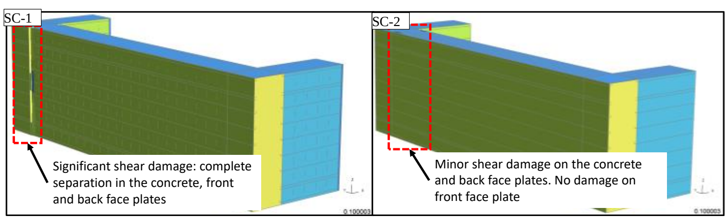

Figure 13. Shear Damage at the end of the simulation time

Figure 14 and Figure 15 present the evolution of the shear damage over time for SC-1 and SC-2 respectively. The figures present the values of the maximum principal strain in the concrete. The damage in the concrete of the SC-1 wall is concentrated in the first 48″ (the first two concrete cells between rib tie plates). After 20msec of loading, the concrete at the connection is significantly damaged and could not transfer shear load to the joint. The bonding studs are completely eroded after 15msec of loading. The combination of these two significant damage states creates vertical crack passing through the front and back face plates at this location of the connection. The face plates could not sustain the magnitude of the load and ruptures after the concrete is significantly damaged. The maximum value for the maximum principal strain in the rib tie plates reached 3% which is lower than the assigned failure criteria (5%) and the rib ties yielded but did not rupture. This is an indication that the rib tie did not reach its maximum capacity during the impact. On the other hand, the SC-2 wall showed a much better performance under high-speed impact. Because the tie rods have smaller spacing, the shear reinforcement interacted early with the concrete in transferring the shear force. As presented in Figure 15, at 10msec, the first row of tie rods rupture after reaching maximum principal strain of 5%. At 15msec, the shear force continues to transfer through the concrete and the tie rods damage extended to the following two rows of ties rods. At 20msec, two more rows are ruptured. The concrete damage is less in SC-2 comparing to SC-1 at all-time steps. This is due to the effective interaction between the tie rods and the concrete at this section. The main reason for having this improved performance at the same reinforcement ratio is due to the closer spacing of the tie rods compared to the rib tie plates, which enhances the force distribution under high-speed impact loading. Another factor is bonding to the concrete. The plate type shear ties have frictional interface with the concrete which does not provide sufficient bonding to the concrete mixture. Accordingly, the shear tension cracks in the concrete are not bridged by the reinforcement. Under the same impacting load, the concrete will fail early in the concrete cell which will form a weak link in the SC wall that will increase its fragility to shear failure. The authors have tested increasing the reinforcement ratio for SC-1 by 50% using 0.75"x16" rib ties. The SC wall fails under the same load with the same pattern, the results could not be presented for sake of brevity in this paper. Additionally, the authors also have investigated shear performance of SC-1 wall using bonded the rib tie plates to the concrete mixture. This could be achieved in construction by adding studs to the rib tie plates. In the FE model the steel plates and the concrete were modeled using common nodes to simulate the bonding. The result for the bonded case is presented in Figure 16 and Figure 17. The connection still observes the same damage as in SC-1 wall without bonded ties. The damage evolution is presented in Figure 16. There is a better stress distribution compared to Figure 14 duo to the bonding, where the damage is stretched over the first two concrete cells. However, the concentration of the damage in the concrete cells still evident.

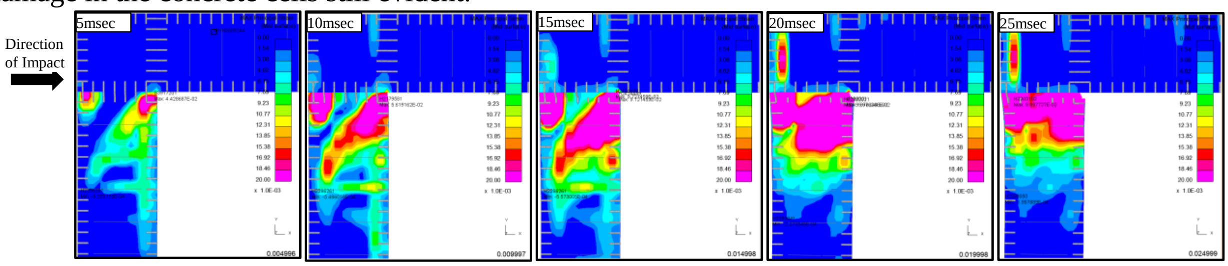

Figure 14. Shear damage evolution over time for SC-1 wall

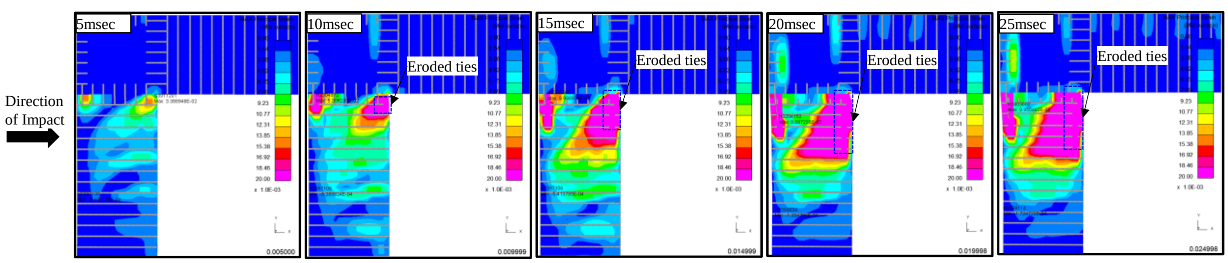

Figure 15. Shear damage evolution over time for SC-2 wall

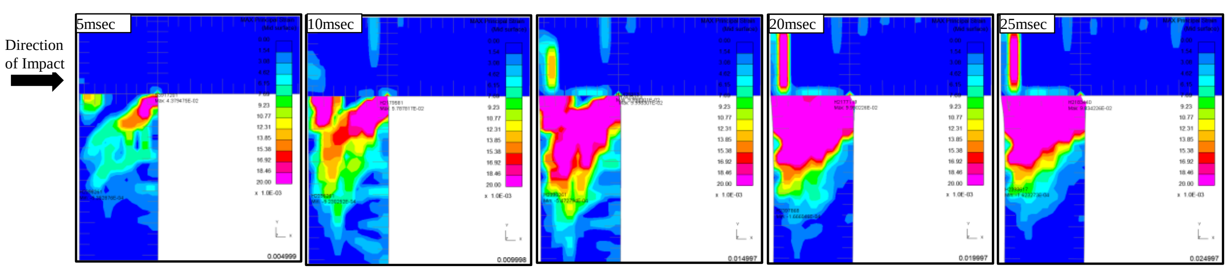

Figure 16. Shear damage evolution over time for SC-1 wall with bonded ties

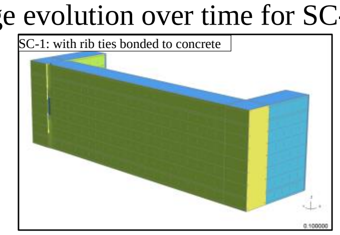

Figure 17. Shear Damage at the end of the simulation time

CONCLUSION

This paper investigated the shear performance of two different type of shear reinforcement under quasi-static loading as well as under high-speed impact loading. The investigated shear reinforcements are rebar type shear reinforcement and plate type shear reinforcement. Under quasi-static loading, the SC-walls adequately follow the AISC-N690 and ACI-349 shear capacity limits. Both reinforcement types show similar shear resistance under quasi-static loading. Under high-speed impact loading, the rebar type shear reinforcement showed much better performance over the plate type shear reinforcement. The smaller spacing of the rebar types of shear reinforcement as well as the bonding between the rebar reinforcement and the concrete mixture provide a better working mechanism under high-speed impact load. For plate type shear reinforcement, the high-speed impact load “pre-maturely” induces excessive damage to the “concrete cell” which is bounded by the rib tie plates. The damaged concrete cell becomes a weak spot in the SC wall and paves the way to initiate a crack in the face plate which is rapidly evolved to form the vertical crack in the SC wall. While rebar type showed better performance, the authors are aware of the construction and fabrication challenges for this type of reinforcement. One potential solution is to utilize a hybrid system, were at the last 2d segment of the wall near the wall-to-wall connection, a rebar type shear reinforcement is used to provide better shear performance, while a plate type shear reinforcement is used elsewhere throughout the wall which is governed by the flexural capacity.

REFERENCES

Broadhouse, B. J. (1986). *DRASTIC: a computer code for dynamic analysis of stress transients in reinforced concrete*. UKAEA Atomic Energy Establishment.

Brown, A. L., Wagner, G. J., & Metzinger, K. E. (2012). Impact, fire, and fluid spread code coupling for complex transportation accident environment simulation. *Journal of Thermal Science and Engineering Applications*, *4*(2).

Japanese Electric Association. (2005). *Technical guidelines for seismic design of steel plate reinforced concrete structures: Buildings and structures*. JEA Tokyo.

Mizuno, J., Koshika, N., Morikawa, H., Fukuda, R., & Wakimoto, K. (2005). *Investigation on impact resistance of steel plate reinforced concrete barriers against aircraft impact Part 2: Simulation analyses of scale model impact tests*.

Mizuno, J., Koshika, N., Sawamoto, Y., Niwa, N., Suzuki, A., & Yamashita, T. (2005). *Investigation on impact resistance of steel plate reinforced concrete barriers against aircraft impact Part 1: Test program and results*.

Mizuno, J., Koshika, N., Tanaka, E., Suzuki, A., Mihara, Y., & Nishimura, I. (2005). *Investigation on impact resistantce of steel plate reinforced conrete barriers against aircraft impact part 3: analyses of full-scale aircraft impact*.

Ottosen, N. S. (1975). *Failure and elasticity of concrete*. Danish Atomic Energy Commission.

Sener, K. C., & Varma, A. H. (2021). Steel-Plate Composite Walls with Different Types of Out-of-Plane Shear Reinforcement: Behavior, Analysis, and Design. *Journal of Structural Engineering*, *147*(2), 04020329.

Sener, K. C., Varma, A. H., & Bhardwaj, S. R. (2015). *Out-of-plane shear strength of SC walls: effects of additional forces*.

Sener, K. C., Varma, A. H., & Seo, J. (2016). Experimental and numerical investigation of the shear behavior of steel-plate composite (SC) beams without shear reinforcement. *Engineering Structures*, *127*, 495–509.

Varma, A. H., Malushte, S. R., Sener, K. C., & Lai, Z. (2014). Steel-plate composite (SC) walls for safety related nuclear facilities: Design for in-plane forces and out-of-plane moments. *Nuclear Engineering and Design*, *269*, 240–249.

Woodfin, R. L. (1983). *Full-scale turbine-missile concrete impact experiments. Final report*. Sandia National Labs.